THE JOURNAL OF BIOLOGICAL CHEMISTRY VOL. 285, NO. 11, pp. 8330–8339, March 12, 2010
© 2010 by The American Society for Biochemistry and Molecular Biology, Inc. Printed in the U.S.A.

Proteasome Assembly Influences Interaction with Ubiquitinated Proteins and Shuttle Factors*[S]

Received for publication, October 17, 2009, and in revised form, December 30, 2009 Published, JBC Papers in Press, January 8, 2010, DOI 10.1074/jbc.M109.076786

Abhishek Chandra, Li Chen, Huiyan Liang, and Kiran Madura[1]

From the Department of Biochemistry, Robert Wood Johnson Medical School, University of Medicine and Dentistry of New Jersey, Piscataway, New Jersey 08854

A major fraction of intracellular protein degradation is mediated by the proteasome. Successful degradation of these substrates requires ubiquitination and delivery to the proteasome followed by protein unfolding and disassembly of the multiubiquitin chain. Enzymes, such as Rpn11, dismantle multiubiquitin chains, and mutations can affect proteasome assembly and activity. We report that different *rpn11* mutations can affect proteasome interaction with ubiquitinated proteins. Moreover, proteasomes are unstable in *rpn11-1* and do not form productive interactions with multiubiquitinated proteins despite high levels in cell extracts. However, increased levels of ubiquitinated proteins were found associated with shuttle factors. In contrast to *rpn11-1*, proteasomes expressing a catalytically inactive mutant (rpn11^{AXA}) were more stable and bound very high amounts of ubiquitinated substrates. Expression of the carboxyl-terminal domain of Rpn11 partially suppressed the growth and proteasome stability defects of *rpn11-1*. These results indicate that ubiquitinated substrates are preferentially delivered to intact proteasome.

A major fraction of intracellular protein degradation is mediated by the proteasome, which consists of a catalytic (20 S) complex that is bound to two regulatory (19 S) particles (1). The 20 S catalytic particle is assembled through a series of intermediates that are guided by chaperones (2–5). In contrast, insight into 19 S particle assembly is only now beginning to emerge (6–12). The 19 S regulatory particle consists of two subcomplexes, base and lid, that are linked by Rpn10 (13), a multiubiquitin chain receptor (14). Recent studies suggest that the assembly of the base subcomplex of the 19 S particle occurs in close association with the 20 S catalytic particle (8). Rpn10 is an important substrate receptor in the proteasome, and its activity is functionally linked to shuttle factors that translocate substrates to the proteasome (15, 16), such as Rad23 (17–19). The loss of both Rpn10 and Rad23 (*rad23*Δ *rpn10*Δ) severely impairs growth and proteolysis (17).

We examined the delivery of ubiquitinated substrates to the proteasome in *rpn11* mutants of *Saccharomyces cerevisiae*. The temperature-sensitive *rpn11-1* (*mpr1-1*) mutant displays growth, proteolytic, and mitochondrial deficiencies (20). Another mutant (*rpn11*^{AXA}), which contains engineered changes in the MPR1-PAD1-N terminas (MPN) domain, does not support viability, although certain biochemical properties have been examined in an *rpn11-1* mutant (21). In agreement with previous studies (21), we found that *rpn11-1* harbors structurally defective proteasomes that showed reduced binding to multiubiquitinated proteins and low peptidase activity. In contrast, proteasomes containing the catalytically inactive rpn11^{AXA} mutant protein are structurally sound and bind very high levels of multiubiquitinated proteins. Expression of the carboxyl terminus of Rpn11 (GST-C^{Rpn11})[2] partially suppressed the diverse defects of *rpn11-1*, consistent with other studies that showed the this domain is required for Rpn11 function (21–23). We found that the high levels of multiubiquitinated proteins in *rpn11-1* were bound to shuttle factors. In contrast, multiubiquitinated proteins that accumulated in rpn11^{AXA} were enriched in proteasomes. One interpretation of these results is that shuttle factors transfer ubiquitinated proteins to intact proteasomes, even if they are functionally defective.

EXPERIMENTAL PROCEDURES

Yeast Strains and Plasmids—RPN11, *rpn11-1*, and *rpn11*^{AXA} were kindly provided by Drs. Deshaies and Verma (California Institute of Technology, Pasadena, CA). Plasmid DNA for generating an integrated derivative of Pre1-FLAG was provided by Dr. J. Dohmen (University of Cologne). DNA was partially digested with BsmI and transformed into the strains indicated in supplemental Table 1. Plasmid DNA for integrating Rpn1-GFP-HA into the chromosomal locus was provided Dr. C. Enenkel (Humboldt University). (Plasmids are indicated in supplemental Table 2.) A plasmid for integrating FLAG-Rpn7 was prepared by amplifying the gene with its native promoter and cloning into Yiplac22 (24). Integrative transformation was performed after the DNA was digested with MscI. To generate a fusion of the carboxyl terminus of Rpn11 with glutathione *S*-transferase (GST), we amplified the DNA encoding amino acids 267–306 and cloned it into pCBGST1 (GST-C^{Rpn11}). Plasmids expressing Rad23, Ddi1, and Dsk2 with an amino-terminal FLAG epitope were generated by PCR and cloned into Yeplac112. These genes were expressed from a P_{CUP1} promoter by the addition of 100 μM $CuSO_4$. All the amplified DNAs were verified by sequencing both strands.

* This work was supported, in whole or in part, by National Institutes of Health Grants CA83875 and GM083321 (to K. M.).

[S] The on-line version of this article (available at http://www.jbc.org) contains supplemental Tables 1 and 2.

[1] To whom correspondence should be addressed: SPH-383, 683 Hoes Lane, Piscataway, NJ 08854. Fax: 732-235-4783; E-mail: maduraki@umdnj.edu.

[2] The abbreviations used are: GST, glutathione *S*-transferase; CP, catalytic (20 S) particle; RP, regulatory (19 S) particle; GFP, green fluorescent protein; HA, hemagglutinin; LLVY-AMC, leucine-leucine-valine-tyrosine-7-amino-4-methylcoumarin; UBA, ubiquitin-associated; UbL, ubiquitin-like; Tricine, *N*-[2-hydroxy-1,1-bis(hydroxymethyl)ethyl]glycine.

Measurement of LLVY-AMC Hydrolysis—Protein lysates (15 μg in 50 μl) were premixed with 200 ng of proteasome inhibitor epoxomicin (Boston Biochem) or an equivalent volume of dimethyl sulfoxide (DMSO) lacking the inhibitor. Proteasome assay buffer (200 μl; 25 mM HEPES, pH 7.5, 0.5 mM EDTA) contained 40 μM LLVY-AMC (Boston Biochem) with or without 0.05% SDS. Reactions were incubated at 30 °C for 1 h, and fluorescence was measured using a Tecan Infinite F200 detector. Similarly, LLVY-AMC hydrolysis by immunopurified proteasomes was performed directly on the FLAG-agarose matrix. The values represent epoxomicin-sensitive measurements that were generated from duplicate assays that were repeated three times.

Growth Assays and Sensitivity to Translation Inhibitors—Yeast cultures were grown in selective medium and normalized to an optical density at A_{600} of ~1. Ten-fold serial dilutions were prepared and spotted on YPD agar plates and then incubated at either 23 °C or 37 °C. Aliquots were also spotted onto medium containing 0.8 mM paromomycin or 0.1 mM hygromycin-B (25).

UV Survival Assays—Yeast strains were grown in synthetic medium (~10^7 cells/ml), washed with sterile water, and resuspended at A_{600} of 1. Ten-fold serial dilutions were spread on YPD plates and exposed to 254-nm UV light at 1 J/m^2/s. The plates were exposed for 0, 30, 60, and 90 s and incubated in the dark at 30 °C. The number of colonies was counted after 4 days, and the average value of duplicate platings from two experiments was plotted.

Pulse-Chase Measurement of Protein Stability—Protein stability measurements were performed as described previously (26, 27) by metabolically labeling yeast cells with 0.5 mCi of EXPRE^{35}S^{35}S (PerkinElmer Life Sciences). Following incubation for 5 min at 30 °C, the cells were suspended in chase medium containing cycloheximide and unlabeled methionine and cysteine. Aliquots were withdrawn at 0, 10, 30, and 60 min. Equal amounts of [^{35}S]cpm were incubated with antibodies against β-galactosidase and protein A-Sepharose. The gels were treated with salicylic acid, dried, and exposed to x-ray film.

Native PAGE—Measurement of peptidase activity of proteasomes was examined in a native polyacrylamide gel, as described (28). Protein lysates (50 μg) were separated in steps of 3, 4, and 5% polyacrylamide and resolved at 4 °C (125 V × 3 h). The gel was overlaid with buffer containing LLVY-AMC, and the fluorescence signal was captured with a Kodak GelLogic imager. Peptidase activity of the 20 S core was stimulated by 0.05% SDS.

Immunoprecipitation/Immunoblotting—Yeast cells were suspended in buffer A (50 mM HEPES, pH 7.5, 150 mM NaCl, 5 mM EDTA and 1% Triton X-100) containing Complete protease inhibitor (Roche) and lysed by glass bead disruption (Thermo-Savant Fast Prep FP120). Protein extracts were normalized using the Bradford reagent (Bio-Rad) and incubated with FLAG-M2 affinity agarose (Sigma). The bound proteins were released in SDS gel loading buffer, separated in 10 or 12% SDS-Tricine PAGE, and characterized by immunoblotting.

Formaldehyde Cross-linking—Cells were grown in YPD medium at 30 °C. Cell pellets were suspended in 1% formaldehyde for 15 min on ice and then washed four times with 1 ml of phosphate-buffered saline.

Antibodies—Polyclonal anti-Rpn12 and anti-Rpn10 antibodies were provided by Dr. D. Skowyra (St. Louis University). Anti-Pab1 was a gift from Dr. S. Peltz (University of Medicine and Dentistry of New Jersey (UMDNJ)). Antibodies against ubiquitin and FLAG were from Sigma. Monoclonal antibodies against β-galactosidase were from Promega (Madison, WI). Antibodies against GST-tagged Rpt1, Rad23, Rpn11, and Dsk2 were made at Pocono Rabbit Farm and Laboratory, Inc. (Canadensis, PA).

Reagents—Epoxomicin and Suc-LLVY-AMC were purchased from Boston Biochem. Enhanced chemiluminescent (ECL) reagents were from PerkinElmer Life Sciences, and the signals were detected using a Kodak GelLogic 1500 imaging system.

RESULTS

Proteasome Assembly Influences Interaction with Multiubiquitinated Proteins—A high copy (2 μM) plasmid expressing Pre1-FLAG, an epitope-tagged subunit in the 20 S catalytic particle, was transformed into yeast strains *RPN11*, *rpn11-1*, and *rpn11*^{AXA}. These strains also contained an integrated, epitope-tagged derivative of Rpn1 (Rpn1-GFP-HA). Yeast strains were grown at the permissive temperature (23 °C), and a part of the culture was transferred to the non-permissive temperature (37 °C) for 4 h. Extracts were prepared, and proteasomes were purified on FLAG-agarose. The precipitated proteins were resolved by SDS-PAGE and examined by immunoblotting (Fig. 1*A*). Incubation of the filter with anti-ubiquitin antibodies showed that proteasomes purified from *rpn11*^{AXA} contained high levels of multiubiquitinated proteins at 23 °C (Fig. 1*A*, *lane 4*). A further increase in the levels of multiubiquitinated proteins was observed at 37 °C (*lane 7*), consistent with the growth and proteolytic defects of this mutant. In contrast, the amount of multiubiquitinated proteins that was co-purified with proteasomes from *rpn11-1* was noticeably reduced (*lanes 3* and *6*). The immunoblots were probed sequentially with antibodies against other proteasome subunits, including Rpn10, Rpn1 (anti-HA), and Rpt1. Intriguingly, although similar levels of Pre1-FLAG were recovered from each strain (*lower panel*, *Pre1*), the amount of 19 S subunits co-purified from *rpn11-1* was significantly lower than from *RPN11* and *rpn11*^{AXA}. Nonspecific precipitation was not detected in a strain lacking Pre1-FLAG (*Ctrl*, *lane 1*).

Our initial studies were performed using yeast strains that overexpressed Pre1-FLAG (Fig. 1*A*). To avoid the possibility that these findings were affected by the high levels of Pre1-FLAG, we generated integrated derivatives of Pre1-FLAG in *RPN11*, *rpn11-1*, and *rpn11*^{AXA} (Fig. 1, *B* and *C*). Protein extracts were prepared from cells grown at 23 and 37 °C, and proteasomes were purified on FLAG-agarose. Total protein extracts were examined by immunoblotting (Fig. 1*B*), and anti-ubiquitin antibodies showed high levels of multiubiquitinated proteins in both *rpn11-1* and *rpn11*^{AXA} at 23 °C (*lanes 2* and *3*) and much higher levels at 37 °C (*lanes 5* and *6*). The immunoblots were probed with antibodies against proteasome subunits (indicated on the *right*). A control reaction (anti-Pab1) revealed

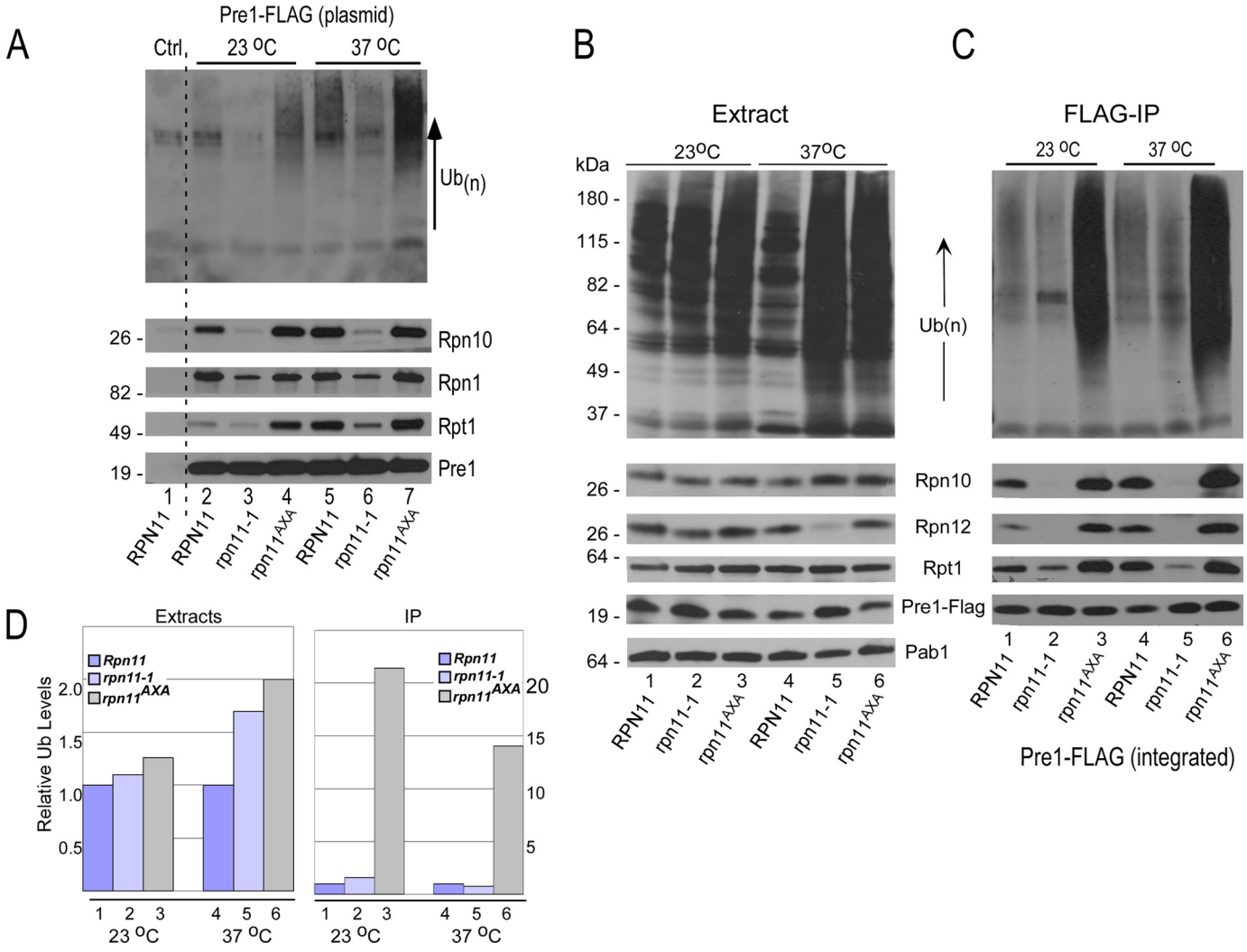

FIGURE 1. **Proteasome assembly affects interaction with multiubiquitinated proteins.** *A*, *RPN11*, *rpn11-1*, and *rpn11*^{AXA} expressing 20 S subunit Pre1-FLAG from a plasmid were grown for 4 h at either 23 °C or 37 °C. An equal amount of protein extract was incubated with FLAG-agarose to purify proteasomes, and the bound proteins were resolved in SDS-10% polyacrylamide gels. Immunoblots were incubated sequentially with antibodies against ubiquitin (*Ub*) (*upper panel*), Rpn10, Rpn1, Rpt1, and Pre1-FLAG. *B*, a gene encoding Pre1-FLAG was integrated into *RPN11*, *rpn11-1*, and *rpn11*^{AXA} and was expressed at physiological levels. Equal amounts of protein extracts were separated by SDS-PAGE and examined with antibodies. A control lane (*Ctrl*) represents the *RPN11* wild-type strain lacking Pre1-FLAG. With the exception of Rpn12, equivalent levels of the other proteasome subunits were detected. *C*, equal amounts of protein extract were incubated with FLAG-agarose, and the bound proteins were resolved by SDS-PAGE. Immunoblots were treated with the antibodies against the indicated proteins. *IP*, immunoprecipitation. *D*, the amount of ubiquitin detected in *panels B* and *C* was quantified by densitometry. The levels of ubiquitin in extracts prepared from *rpn11-1* and *rpn11*^{AXA} were compared with *RPN11* (where the value is set to 1). The levels of ubiquitin in proteasomes purified from *rpn11-1* and *rpn11*^{AXA} are also compared with *RPN11* (where the amount is arbitrarily set to 1).

equal protein loading. Despite moderate variability in Pre1-FLAG levels, the overall abundance of other proteasome subunits was similar, with the exception of Rpn12, whose levels were significantly reduced in *rpn11-1* at 37 °C (*lane 5*).

Protein extracts were applied to FLAG-agarose to purify proteasomes (Fig. 1*C*). Very low amounts of multiubiquitinated species were isolated in association with proteasomes purified from *rpn11-1* (*lanes 2* and *5*), despite the high levels that were detected in total extracts (Fig. 1*B*). This is evident when Fig. 1*B*, *lanes 4* and *5*, are compared with Fig. 1*C*, *lanes 4* and *5*. Rpn10 and Rpn12 were not co-purified with proteasomes from *rpn11-1* at either 23 °C (*lane 2*) or 37 °C (*lane 5*). Similarly, the ATPase subunit Rpt1 was inefficiently purified with proteasomes at 23 °C (*lane 2*) and 37 °C (*lane 5*). These results reveal a faulty interaction between the 20 S particle and components of the 19 S particle in *rpn11-1*. The high levels of multiubiquitinated proteins that were purified with proteasomes in *rpn11*^{AXA} (*lanes 3* and *6*) could reflect higher levels in total extract (Fig. 1*B*, *lanes 3* and *6*), as well as more stable proteasomes (Fig. 1*C*, *lanes 3* and *6*). Equivalent amount of Pre1-FLAG was isolated from each strain, indicating that the results are not caused by variable abundance of the 20 S particle.

The levels of high molecular weight multiubiquitinated proteins shown in Fig. 1, *B* and *C*, were quantified (Fig. 1*D*). The densitometry results do not fully reflect the magnitude of difference in total multiubiquitin levels in *rpn11-1* and *rpn11*^{AXA} due to saturation of the signal in Fig. 1*B*. Nonetheless, the quantified data clearly show that the amount of ubiquitinated proteins that were co-purified with proteasomes from *rpn11*^{AXA} was ~20-fold higher than in *rpn11-1*.

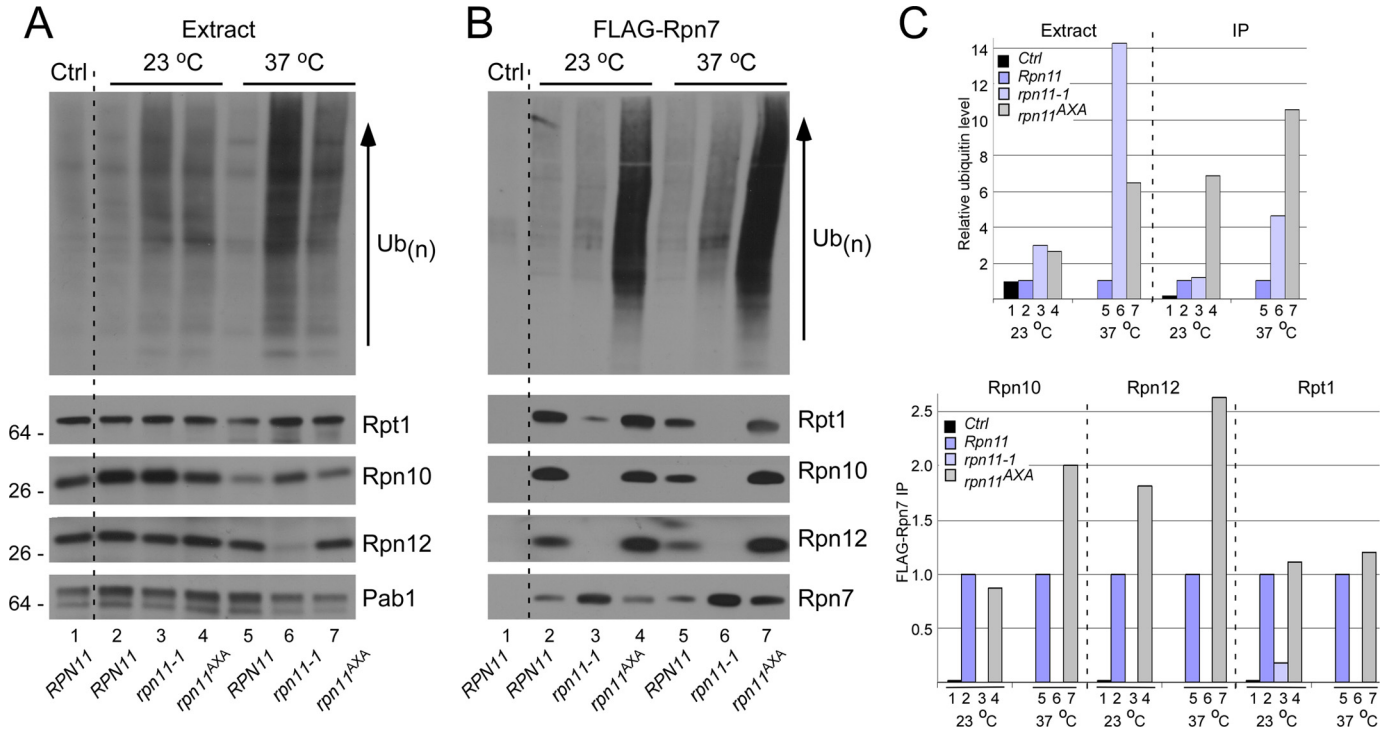

FIGURE 2. **Proteasomes purified with a lid subunit show assembly defects in *rpn11-1*.** *A*, a FLAG epitope-tagged derivative of Rpn7 was inserted into the chromosomal locus in *RPN11*, *rpn11-1*, and *rpn11*^{AXA} and expressed at physiological levels. Total protein extracts were prepared from strains grown at 23 and 37 °C and examined by immunoblotting. *Lane 1* contains extract prepared from a wild-type strain lacking a FLAG-tagged protein (*Ctrl*). The level of Rpn12 is lower in *rpn11-1* at 37 °C (*lane 6*). The reaction against Pab1 represents a protein loading control. *Ub*, ubiquitin. *B*, FLAG-Rpn7 was immunoprecipitated on FLAG-agarose, and the bound proteins were examined by immunoblotting with antibodies against the proteins indicted on the *right*. The control lane (*Ctrl*, *lane 1*) shows no reaction against any of the proteasome subunits. The expression of FLAG-Rpn7 is shown in the *bottom panel*. Despite the recovery of high levels of FLAG-Rpn7 from *rpn11-1* at 37 °C, 19 S subunits were not co-purified (*lane 6*). *C*, the levels of ubiquitin cross-reacting material in *panels A* and *B* were quantified by densitometry (*upper panel*). Ubiquitin levels in *lane 1* (*Ctrl*) were set to an arbitrary value of 1. The *lower panel* shows the quantified levels of proteasome subunits Rpn10, Rpn12, and Rpt1 from *panel B*. For each protein, the signal in the wild-type strain is set to 1. *IP*, immunoprecipitation.

Proteasomes Purified with a Lid Subunit Confirmed an Assembly Defect in rpn11-1—The results in Fig. 1 suggested that the association between 19 S and the 20 S particles is significantly reduced in *rpn11-1*. To corroborate these findings, we integrated a lid subunit, FLAG-Rpn7, in *RPNP11*, *rpn11-1*, and *rpn11*^{AXA}. Protein extracts were prepared from cultures grown at 23 and 37 °C (for 4 h) and examined by immunoblotting. A control strain lacking FLAG-Rpn7, and the same strain containing integrated FLAG-Rpn7, showed low levels of multiubiquitinated proteins in total extracts (Fig. 2*A*, *lanes 1* and *2*). The levels of Rpt1, Rpn10, and Rpn12 were also similar in these two strains, demonstrating that the expression of FLAG-Rpn7 had no adverse effects on proteasome abundance. High levels of multiubiquitinated proteins were detected in total extracts prepared from *rpn11-1* and *rpn11*^{AXA} at both 23 °C (*lanes 3* and *4*) and 37 °C (*lanes 6* and *7*). As noted earlier, the abundance of Rpn12 was significantly reduced in *rpn11-1* at 37 °C (Fig. 2*A*, *lane 6*). Pab1 levels provide a loading control (*bottom panel*).

FLAG-Rpn7 was immunoprecipitated to investigate proteasome composition (Fig. 2*B*). Large amounts of multiubiquitinated proteins were co-purified with FLAG-Rpn7 from *rpn11*^{AXA} at both 23 °C (*lane 4*) and 37 °C (*lane 7*). However, the amount of Rpt1, Rpn10, and Rpn12 that was co-purified with FLAG-Rpn7 from *RPN11* and *rpn11*^{AXA} was similar despite the strikingly different amounts of associated multiubiquitinated proteins (compare *lanes 2* and *4*). Although high amounts of FLAG-Rpn7 were immunoprecipitated from *rpn11-1* (Fig. 2*B*, *lane 3* and *6*, *bottom panel*), very low levels of Rpt1, Rpn10, Rpn12, and multiubiquitinated proteins were recovered.

The levels of ubiquitinated species were quantified by densitometry (Fig. 2*C*). Wild-type yeast, either lacking or expressing integrated FLAG-Rpn7, contained equivalent amounts of ubiquitin cross-reacting material at 23 °C (Extract, *lanes 1* and *2*) and 37 °C (*lane 5*). However, high levels were measured in *rpn11-1* and *rpn11*^{AXA}. The amount of ubiquitinated proteins that was immunoprecipitated with FLAG-Rpn7 from *rpn11*^{AXA} was significantly increased at both 23 °C (*IP*, *lane 4*) and 37 °C (*lane 7*). The co-purification of Rpn10, Rpn12, and Rpt1 with FLAG-Rpn7 was also quantified (Fig. 2*C*, *lower panel*).

Proteasome Stability Is Reduced in rpn11-1—The failure to purify 19 S subunits from *rpn11-1*, using Pre1-FLAG (Fig. 1*C*) or FLAG-Rpn7 (Fig. 2*B*), suggested that proteasomes might be unstable in this mutant. Because proteasomes are essential for viability, the apparent dissociation is likely to occur during purification. A similar instability of 19 S particle was previously detected in *rpn10*Δ (13). To test this idea, yeast cells were grown at 23 °C and treated with formaldehyde to cross-link proteasome subunits and associated factors (Fig. 3). Total protein extracts were prepared from *RPN11*, *rpn11-1*, and *rpn11*^{AXA} containing integrated Pre1-FLAG, as well as a control strain lacking Pre1-FLAG (*Ctrl*, *lanes 1* and *2*). Extracts were prepared from untreated and formaldehyde-treated cells and examined

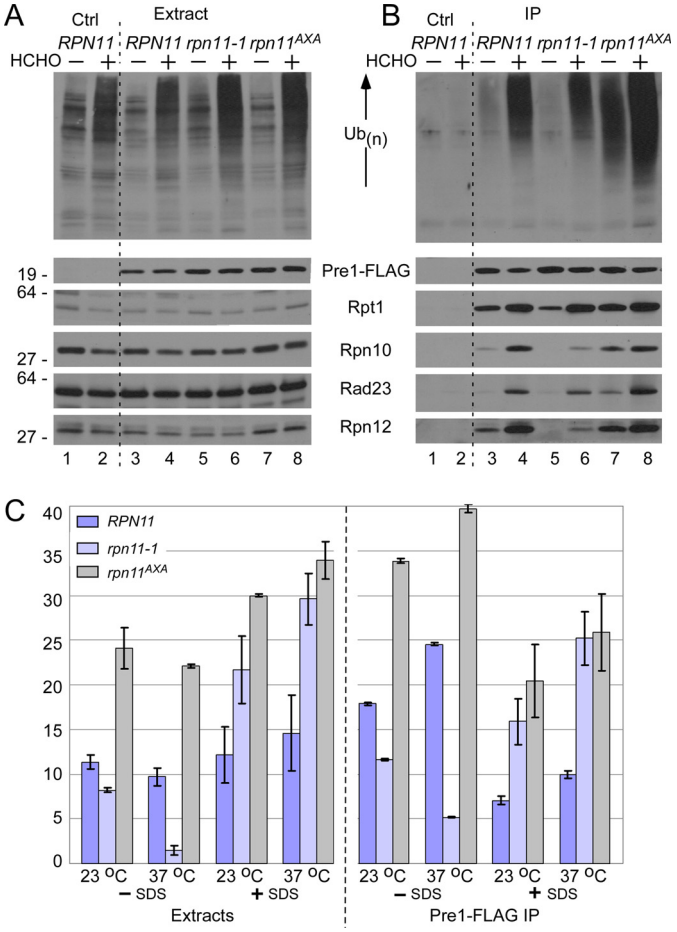

FIGURE 3. **Proteasome stability is reduced in *rpn11-1*.** *A*, actively growing *RPN11*, *rpn11-1*, and *rpn11*^{AXA} yeast strains expressing Pre1-FLAG at physiological levels were suspended in medium containing 1% formaldehyde (*HCHO*) on ice. Protein extracts were prepared from untreated and treated cells and resolved by SDS-PAGE. An immunoblot was incubated with antibodies against the proteins indicated on the *right*. A strain lacking Pre1-FLAG is shown in *lanes 1* and *2*. A control lane (*Ctrl*) represents the *RPN11* wild-type strain lacking Pre1-FLAG. *B*, protein extracts were incubated with FLAG-agarose to immunoprecipitate (*IP*) Pre1-FLAG and proteasome-associated Rpt1, Rpn10, Rpn12, and the shuttle factor Rad23. The *upper panel* shows the levels of multiubiquitinated proteins that were recovered in each strain. No proteasome subunits were isolated from a strain lacking Pre1-FLAG (*lanes 1* and *2*). *Ub*, ubiquitin. *C*, chymotryptic peptidase activity of proteasomes isolated from *RPN11*, *rpn11-1*, and *rpn11*^{AXA} was measured using the fluorogenic substrate LLVY-AMC. Protein extracts were prepared from cells grown at either 23 °C or 37 °C and measured in the presence or absence of 0.05% SDS. Epoxomicin-sensitive values were determined in duplicate. The *right panel* represents activity that was co-precipitated with Pre1-FLAG. *Error bars* represent S.D.

by immunoblotting. The levels of proteasome subunits (Rpt1, Rpn12, and Rpn10), and a shuttle factor (Rad23) were unchanged upon formaldehyde treatment (Fig. 3*A*). Although Pre1-FLAG was expressed at equivalent levels (Fig. 3*A*, *lanes 3–8*), multiubiquitinated proteins were detected at significantly higher levels in the formaldehyde-treated cell extracts (*upper panel*). The levels detected in *rpn11-1* and *rpn11*^{AXA} were higher than in *RPN11* (*lanes 6* and *8*).

Pre1-FLAG was immunoprecipitated from untreated and formaldehyde-treated cells, and the co-purified proteins were examined by immunoblotting (Fig. 3*B*). Nonspecific precipitation of proteasome subunits or multiubiquitinated proteins was not observed in the control strain (*Ctrl*, *lanes 1* and *2*), demonstrating the effectiveness of the procedure and the specificity of the antibody reaction. Similar amounts of Pre1-FLAG were recovered from all strains, in both treated and untreated preparations. High levels of multiubiquitinated proteins were co-purified with proteasomes from wild-type cells following formaldehyde treatment (compare *lanes 3* and *4*). High levels of multiubiquitinated proteins were purified with proteasomes from *rpn11*^{AXA}, both in the presence and in the absence of cross-linking (*lanes 8* and *7*). The co-purification of Rpn10, Rpn12, and Rad23 with proteasomes from *rpn11*^{AXA} was similarly elevated. Significantly, chemical cross-linking allowed us to detect proteasome subunits and ubiquitinated proteins in proteasomes isolated from *rpn11-1* (compare *lanes 5* and *6*). This finding is consistent with the idea that proteasomes are unstable in *rpn11-1*.

The base subcomplex of the 19 S particle can regulate protein degradation by controlling the translocation of substrates into the 20 S particle (29–32). However, the peptidase activity of the free 20 S particle can also be stimulated by low concentration of detergent. We measured peptidase activity to determine whether the altered stability of proteasomes in *rpn11-1* affected its catalytic function. Protein extracts were prepared from *RPN11*, *rpn11-1*, and *rpn11*^{AXA} and incubated with LLVY-AMC to measure chymotryptic activity (Fig. 3*C*). Although proteasomes are equally abundant in *RPN11* and *rpn11*^{AXA} (Fig. 3*A*), peptidase activity was noticeably higher in *rpn11*^{AXA} at both 23 °C and 37 °C. The chymotryptic activity in *rpn11-1* was similar to the wild type at 23 °C but was significantly reduced at 37 °C. We speculate that high temperature might further destabilize proteasomes in *rpn11-1*, leading to reduced hydrolysis of LLVY-AMC. We measured proteasome activity in *rpn11-1* extracts after the addition of SDS and detected ~4- and ~15-fold higher levels at 23 and 37 °C. We propose that proteasome dissociation in *rpn11-1* might result in the accumulation of 20 S particles. SDS-stimulated activity was also higher in *rpn11*^{AXA} than in *RPN11*, demonstrating that both mutants retained robust hydrolytic activity.

Protein extracts were incubated with FLAG-agarose, and peptidase activity that was purified with Pre1-FLAG was measured. In the absence of SDS, proteasomes purified from *rpn11-1* showed slightly lower peptidase activity than in wild-type proteasomes (at 23 °C). However, peptidase activity was markedly reduced at 37 °C, consistent with the increased instability of proteasomes in *rpn11-1* at higher temperature. Proteasomes purified from *rpn11*^{AXA} showed high chymotryptic activity at both 23 °C and 37 °C. At 37 °C, peptidase activity of *rpn11*^{AXA} proteasomes was almost 8-fold higher than *rpn11-1* proteasomes. The addition of SDS resulted in higher activity in both *rpn11-1* and *rpn11*^{AXA} proteasomes when compared with *RPN11*. However, an overall decrease in LLVY-AMC hydrolysis (when compared with extract) could be due to an inhibitory effect of SDS on immobilized proteasomes (see Fig. 7*C*). Nonetheless, the pattern of peptidase activities in the three strains, in the presence or absence of SDS, is similar in extracts and purified proteasomes.

Autonomous Expression of Carboxyl-terminal Residues Can Partially Suppress the Defects of rpn11-1—The defects of *rpn11-1* are caused by the loss of 31 residues from the carboxyl

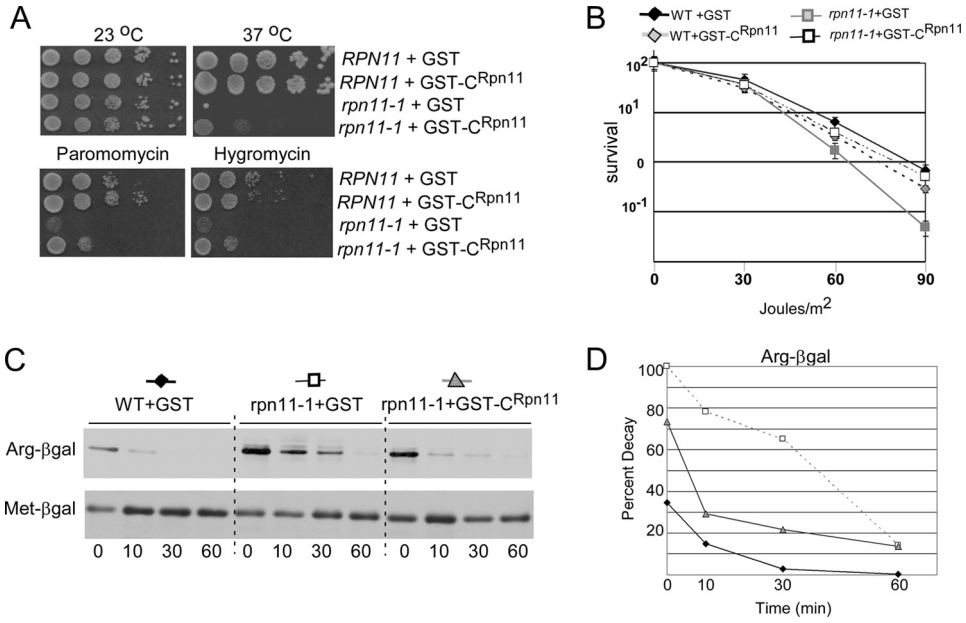

FIGURE 4. **Autonomous expression of carboxyl-terminal residues of Rpn11 can partially suppress the defects of *rpn11-1*.** *A*, the carboxyl terminus of Rpn11 was expressed as a fusion with glutathione *S*-transferase (GST-C^{Rpn11}) in *RPN11* and *rpn11-1*. Ten-fold dilutions of yeast cells expressing either GST or GST-C^{Rpn11} were spotted on agar medium, and suppression of *rpn11-1* phenotypes was determined. *B*, the UV sensitivity of *RPN11* and *rpn11-1*, containing either GST or GST-C^{Rpn11}, was measured. Exponential phase yeast cells were diluted and plated on agar medium and exposed to 254-nm UV light at a fluence of 1 J/m^2/s. Survival was determined following 4 days of incubation at 23 °C in the dark. The figure is representative of two independent experiments. *Error bars* represent S.D. *WT*, wild type. *C*, *RPN11* expressing GST and *rpn11-1* expressing either GST or GST-C^{Rpn11} were transformed with plasmids expressing the engineered substrate Arg-β-galactosidase (*Arg-βgal*) or the stable protein Met-β-galactosidase (*Met-βgal*). *In vivo* stability of these proteins was measured in a [^{35}S]methionine pulse-chase experiment. Radiolabeled proteins were immunoprecipitated and resolved by SDS-PAGE, and the autoradiographic data were quantified (*panel D*).

terminus. We investigated whether the expression of this domain in *trans* could alleviate the growth and proteolytic defects of *rpn11-1*. A recent study showed that the C-terminal one-third of Rpn11 could overcome the mitochondrial and DNA repair defects of *rpn11-1* (22) but not its proteolytic deficiency. We expressed the carboxyl-terminal 39 residues of rpn11-1 (GST-C^{Rpn11}) in *RPN11* and *rpn11-1* (Fig. 4). GST-C^{Rpn11} did not cause any adverse effects in the wild-type strain. Ten-fold dilutions were spotted onto agar-containing medium and incubated at either 23 °C or 37 °C. The temperature-sensitive growth defect of *rpn11-1* was partially suppressed by GST-C^{Rpn11} but not by GST (Fig. 4*A*). GST-C^{Rpn11} also enabled growth at the semipermissive temperature (30 °C) on medium containing the translational inhibitors paromomycin and hygromycin-B. Both drugs generate high levels of damaged proteins and provide a rapid way to examine proteolytic proficiency (25). The partial suppression of the growth defect of *rpn11-1* by GST-C^{Rpn11} was accompanied by a moderate recovery of proteasome function (see Fig. 5). The UV sensitivity of *rpn11-1* was restored to wild-type levels by GST-C^{Rpn11} (Fig. 4*B*), consistent with a recent report that showed that the carboxyl-terminal 100 amino acid residues suppressed the methyl methane sulfonate sensitivity of *rpn11-1* (23). To measure proteolytic activity, we transformed *RPN11* and *rpn11-1* with plasmids encoding the proteolytic substrate Arg-β-galactosidase or a control protein Met-β-galactosidase (26). We also expressed GST in *RPN11* and either GST or GST-C^{Rpn11} in *rpn11-1*. GST had no effect on the stability of Arg-β-galactosidase in the wild-type strain (*RPN11*). Arg-β-galactosidase was stabilized in *rpn11-1* containing GST (Fig. 4*C*, *middle panel*), but degradation was partially restored by expressing GST-C^{Rpn11}. The half-life of Arg-β-galactosidase was determined to be <5 min in the wild-type strain and ~30 min in *rpn11-1*. Expression of GST-C^{Rpn11} reduced the stability of Arg-β-galactosidase to ~10 min.

The Carboxyl Terminus of Rpn11 Promotes Proteasome Stability—The suppression of *rpn11-1* defects by GST-C^{Rpn11} could be due to increased stability of proteasomes in this mutant. We therefore examined the integrity of proteasomes in *RPN11*, *rpn11-1*, and *rpn11*^{AXA} using a well described in-gel activity assay. Protein extracts were resolved in a native gel in the presence of ATP and incubated in buffer containing LLVY-AMC (Fig. 5). The hydrolysis of this substrate releases a localized fluorescent signal that can provide qualitative data on the levels of intact proteasomes, as well as assembly intermediates. Proteasomes isolated from *rpn11-1* were primarily dissociated or present in altered structural form (Fig. 5*A*, *lane 2*) (21, 23). An immunoblot probing for Pre1-FLAG showed higher levels of the free 20 S catalytic particle (CP) in *rpn11-1* (*lower panel*). The peptidase activity in *rpn11*^{AXA} was detected primarily in the slow migrating form, representing a 20 S complex bound to one (RP1CP) or two regulatory particles (RP2CP), verifying the increased abundance of the intact proteasomes in this mutant.

To determine whether the partial suppression of the growth and proteolytic defects of *rpn11-1* by GST-C^{Rpn11} was due to improved proteasome assembly, we examined its integrity using an in-gel assay. Wild-type (*RPN11*) proteasomes were detected predominantly as RP1CP and RP2CP (Fig. 5*B*) in the presence of either GST or GST-C^{Rpn11} (*lanes 1* and *2*). The expression of GST-C^{Rpn11} in *rpn11-1* noticeably improved the level of intact proteasomes (*lane 4*), although it was not restored to wild-type levels. Proteasomes in *rpn11*^{AXA} were highly active (*lane 6*), and the expression of GST-C^{Rpn11} had no effect (data not shown). Interestingly, overexpressing full-length FLAG-Rpn11 in *rpn11-1* yielded peptidase activity that was higher than in *RPN11* (compare *lanes 1* and *5*). The signals detected in Fig. 5*B* were quantified using data from two independent studies (Fig. 5*C*). The *lightly shaded part* of the column represents activity detected in the absence of SDS, whereas the SDS-induced activity is represented by the *dark shaded part* of the column. The very low level of proteasome activity in *rpn11-1*, in the absence of SDS, is clearly evident.

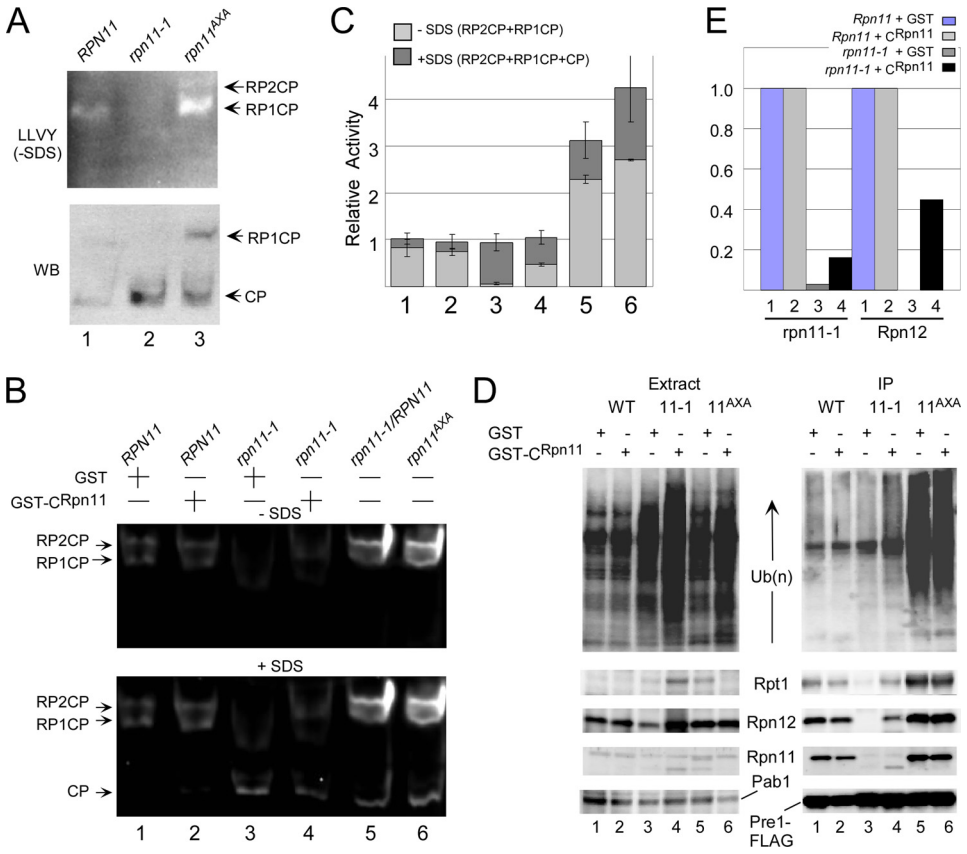

FIGURE 5. **The carboxyl terminus of Rpn11 increases the levels of intact proteasomes.** *A*, we used a fluorogenic assay to measures the cleavage of LLVY-AMC in wild type, *rpn11-1*, and *rpn11*^{AXA}. Proteasomes appear unstable or poorly assembled in *rpn11-1*, as judged by the high levels of free catalytic 20 S particles and low levels of intact proteasomes (*upper panel*, *lane 2*). Proteins resolved in the native gel were transferred to nitrocellulose and then probed with antibodies against the 20 S subunit Pre1-FLAG (*lower panel*, *WB*). *B*, to determine the mechanism of suppression of *rpn11-1* by GST-C^{Rpn11}, peptidase activity was measured in *RPN11* and *rpn11-1* extracts containing either GST or GST-C^{Rpn11}. The level of intact proteasomes was partially restored in *rpn11-1* expressing GST-C^{Rpn11} but not GST (*lane 4*). Expression of the full-length FLAG-Rpn11 protein in *rpn11-1* resulted in complete recovery of proteasome assembly and activity (*lane 5*, FLAG-Rpn11). Total chymotryptic activity was also measured in *rpn11*^{AXA}, and high peptidase activity and increased levels of intact proteasomes were observed. The positions of 20 S particle bound to one or two regulatory particles (RP1CP and RP2CP) are indicated. Activation of the free 20 S particle by SDS is shown in the *lower panel* (*CP*). *C*, the fluorescent signals in *panel B* were quantified. The *lightly shaded bar* represents the activity of proteasomes in the absence of SDS, whereas the addition of the *dark shaded region* represents the total chymotryptic activity that was detected upon the addition of SDS. *Error bars* represent S.D. *D*, the suppression of *rpn11-1* defects by GST-C^{Rpn11} is associated with the partial restoration of intact proteasomes. Pre1-FLAG was immunoprecipitated, and the expression of 19 S proteasome subunits in total extract is shown in the *left panel*. Proteasomes were purified on FLAG-agarose, and the 19 S subunits Rpt1, Rpn12, and Rpn11 were detected in proteasomes isolated from *rpn11-1* (*right panel*, compare *lanes 3* and *4*). *WT*, wild type. *E*, the effect of GST-C^{Rpn11} on proteasome assembly in *rpn11-1* was quantified. The co-precipitation of native rpn11-1 and Rpn12 proteins with Pre1-FLAG was compared in wild-type and *rpn11-1* cells expressing either GST or GST-C^{Rpn11} (shown in *panel D*, *lanes 1–4*).

The effect of the GST-C^{Rpn11} on proteasome stability was also investigated by immunoprecipitating Pre1-FLAG (Fig. 5*D*). The overall levels of multiubiquitinated proteins remained elevated in *rpn11-1* expressing either GST or GST-C^{Rpn11} (see *lanes 3* and *4*). However, in the presence of GST-C^{Rpn11}, low levels of multiubiquitinated proteins were detected in proteasomes purified from *rpn11-1* (*IP*, *right panel*, compare *lanes 3* and *4*). GST-C^{Rpn11} did not have a discernible effect in *rpn11*^{AXA} (compare *lanes 5* and *6*). The filter was also incubated with antibodies against Rpt1, Rpn12, and Rpn11, and low levels were detected in proteasomes purified from *rpn11-1* expressing GST-C^{Rpn11} but not GST (Fig. 5*D*, *IP*, compare *lanes 3* and *4*). Intriguingly, the truncated rpn11-1 protein was detected in proteasomes purified from *rpn11-1* (*lane 4*). These data were quantified by densitometry (Fig. 5*E*), and the improved stability of proteasomes was demonstrated by the recovery of Rpn12 with Pre1-FLAG from *rpn11-1* only in cells expressing GST-C^{Rpn11}.

Substrate Shuttle Factors Show Differential Binding to Proteasomes in rpn11-1 and rpn11^{AXA}—Although high levels of multiubiquitinated proteins were present in *rpn11-1* and *rpn11*^{AXA}, the distinct stabilities of proteasomes in these mutants resulted in dissimilar interaction with ubiquitinated proteins. Specifically, proteasomes purified from *rpn11*^{AXA} contained very high levels of multiubiquitinated substrates (Fig. 1), whereas reduced levels were recovered in *rpn11-1*. Because shuttle factors play a key role in the delivery of proteolytic substrates to the proteasome (33), we examined their interaction with substrates and the proteasome in *rpn11-1* and *rpn11*^{AXA}. The best described shuttle factors resemble Rad23, which contains an amino-terminal ubiquitin-like (UbL) domain that interacts with the proteasome (34) and ubiquitin-associated (UBA) domains that bind multiubiquitin chains (35, 36). These features enable UbL-UBA shuttle factors to deliver substrates through transient interaction with Rpn1 in the base of the proteasome (38) followed by release and recycling.

Dsk2 plays an overlapping role with Rad23 (37). Both proteins were expressed at physiological levels, and their interaction with the proteasome was examined in *RPN11*, *rpn11-1*, and *rpn11*^{AXA} containing integrated Pre1-FLAG. Protein extracts were examined by immunoblotting with antibodies against Rpt1, Rad23, Dsk2, and Pab1 (Fig. 6*A*). The expression of Pre1-FLAG was similar in *RPN11*, *rpn11-1*, and *rpn11*^{AXA} strains at both 23 °C and 37 °C (data not shown). Equivalent expression of Rpt1 and the shuttle factors Rad23 and Dsk2 were detected at 23 and 37 °C in total protein extracts (Fig. 6*A*). Moreover, the amount of Rad23 and Dsk2 that was co-purified with proteasomes at 23 °C was similar in *RPN11*, *rpn11-1*, and *rpn11*^{AXA} (Fig. 6*B*). However, the level of both shuttle factors in proteasomes was strongly decreased in *rpn11-1* at 37 °C (compare *lanes 2* and *5*), whereas their association with proteasomes from *rpn11*^{AXA} at 37 °C was unaffected. Although equivalent amounts of Pre1-FLAG were immunoprecipitated from each strain, significantly lower

amounts of Rpt1 were co-precipitated with the proteasome from *rpn11-1*.

The UbL-UBA shuttle factors bind the Rpn1 subunit in the base complex (38), which also contains the hexameric ring of ATPases that binds the 20 S particle. However, we found that lower amounts of Rpn1 (Fig. 1*A*) and Rpt1 (Fig. 6*B*) were recovered with Pre1-FLAG in *rpn11-1*, which could underlie the reduced proteasome interaction with shuttle factors. Rpt1 was efficiently recovered with proteasomes in *rpn11*^{AXA}, consistent with the high levels of ubiquitinated proteins and shuttle factors that were observed (Fig. 6*B*, and see Fig. 7).

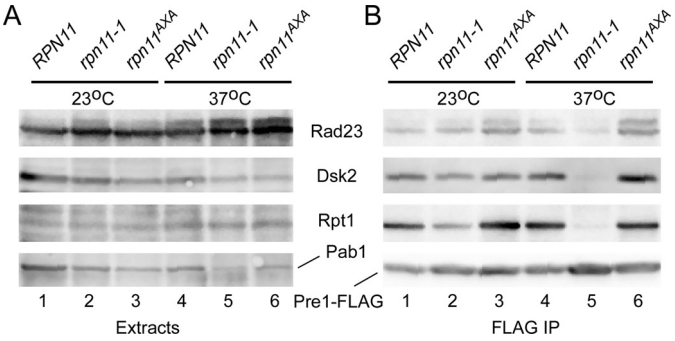

FIGURE 6. **Substrate shuttle factors show differential binding to proteasomes in *rpn11-1* and *rpn11*^{AXA}.** *A*, the interaction between proteasomes and shuttle factors (Rad23 and Dsk2) was determined by immunoprecipitating Pre1-FLAG. Yeast cells were grown at 23 and 37 °C, and total protein extracts were examined. *B*, proteasomes were immunoprecipitated (*IP*) on FLAG-agarose, and the levels of Rad23, Dsk2, and Rpt1 were determined by immunoblotting.

High Levels of Multiubiquitinated Proteins Remain Bound to Shuttle Factors in rpn11-1—Studies described here reveal a failure of multiubiquitinated proteins to be efficiently delivered to or retained on proteasomes in *rpn11-1*. The accumulation of high levels of ubiquitinated proteins in total cell extracts in *rpn11-1* was unexpected because multiubiquitin chains can be rapidly dismantled. However, an interaction with UBA domains in shuttle factors, such as Rad23, can reduce the disassembly of multiubiquitin chains (39). Therefore, we investigated whether multiubiquitinated proteins accumulated on shuttle factors in *rpn11-1*. *RPN11*, *rpn11-1*, and *rpn11*^{AXA} were transformed with plasmids expressing FLAG-Rad23, FLAG-Ddi1, and FLAG-Dsk2. Protein extracts were incubated with FLAG-agarose, and the bound proteins were resolved by SDS-PAGE and transferred to nitrocellulose. Incubation of the filter with anti-ubiquitin antibodies revealed strong interaction with shuttle factors in *rpn11-1* extracts (Fig. 7*A*, *lanes 5*, *8*, and *11*).

To further test these findings, we measured peptidase activity that was purified with the shuttle factors as this would provide an independent gauge of their ability to bind proteasomes. Protein extracts were prepared in the presence of ATP to minimize proteasome disassembly. Shuttle factors were recovered on FLAG-agarose, and the affinity beads were incubated with LLVY-AMC to measure chymotryptic activity. In the absence of SDS, peptidase activity in total extract was lower in *rpn11-1* but significantly higher in *rpn11*^{AXA} (Fig. 7*B*). However, the addition of SDS stimulated the chymotryptic activity in all three strains and was particularly robust in *rpn11-1* (consistent with Fig. 3*C*). This result supports the idea that higher levels of free 20 S catalytic particles accumulate in *rpn11-1* as its activity can be stimulated by SDS. Protein extracts were applied to FLAG-agarose to measure the peptidase activity in proteasomes that were co-purified with the shuttle factors (Fig. 7*C*). As expected, no activity was detected in a strain that did not express a FLAG-tagged protein (vector). Significant chymotryptic activity was immunopurified with FLAG-Rad23 from *RPN11* and *rpn11*^{AXA} in the absence of SDS. In contrast, very low peptidase activity was immunopurified with FLAG-Rad23 from *rpn11-1*. The addition of SDS resulted in a similar trend in chymotryptic activity, although the magnitude of hydrolysis was reduced. We believe that this might be due to an adverse effect of detergent on the affinity matrix. Purification of FLAG-Ddi1 yielded very low activity, consistent with the absence of significant interaction with proteasomes (Fig. 7*A*). In contrast, FLAG-Dsk2 gave qualitatively simi-

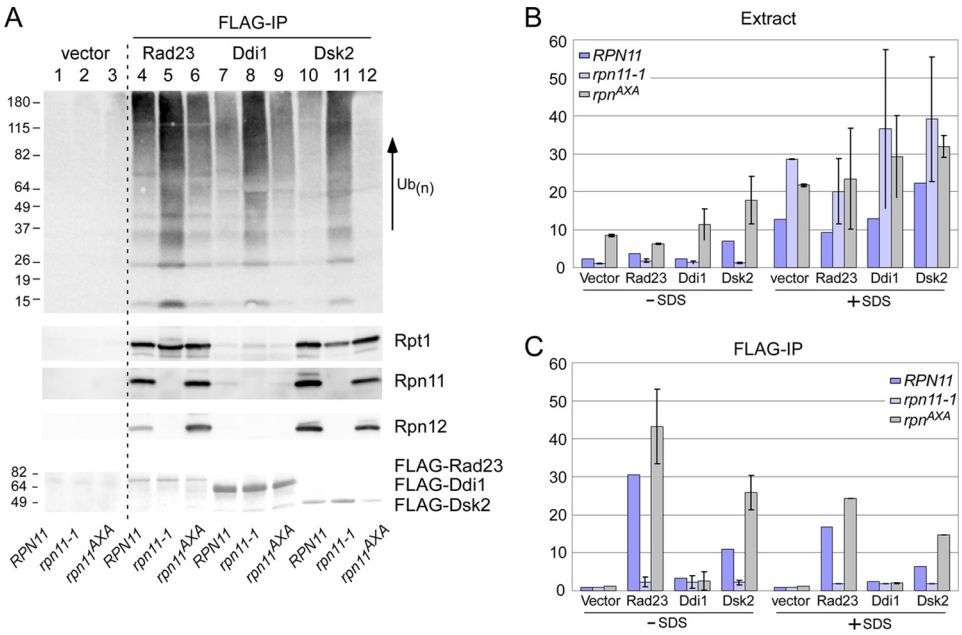

FIGURE 7. **High levels of multiubiquitinated proteins are bound to shuttle factors in *rpn11-1*.** *A*, FLAG-tagged Rad23, Ddi1, and Dsk2 were expressed in *RPN11*, *rpn11-1*, and *rpn11*^{AXA}. A wild-type strain lacking a FLAG-tagged protein was also examined (*vector*, *lanes 1–3*). Protein extracts were incubated with FLAG-agarose, and the levels of multiubiquitinated proteins and proteasome subunits (Rpt1, Rpn11, and Rpn12) that were purified with the shuttle factors were determined. The *lower panel* shows the levels of the shuttle factors by Ponceau S staining. The levels of multiubiquitinated proteins and proteasome subunits Rpt1, Rpn11, and Rpn12 are shown. *IP*, immunoprecipitation. *B*, chymotryptic activity was measured in extracts, in the presence and absence of SDS. In these assays, the extracts were prepared from yeast cells grown at 30 °C to permit semipermissive growth for *rpn11-1* and *rpn11*^{AXA}. *C*, the same extracts were incubated with FLAG-agarose, and peptidase activity co-precipitated with the shuttle factors was determined. (The assays were performed in duplicate.) *Error bars* in *panels B* and *C* represent S.D.

lar results to FLAG-Rad23, suggesting that the stability defect of *rpn11-1* proteasomes affects its interactions with multiple UbL/UBA shuttle factors.

DISCUSSION

The role of chaperones in promoting the assembly of the 20 S catalytic particle has been characterized extensively (2–5). In contrast, knowledge of 19 S complex assembly (6–12) and 26 S maturation is only now emerging. The 19 S base subcomplex was recently reported to occur through a succession of intermediate structures, with the 20 S particle serving as a platform for assembly (8). The ensuing recruitment of a preformed lid complex could yield a complete proteasome.

Mutation in the Rpn11 deubiquitinating enzyme can affect proteasome assembly (21, 23) and interaction with multiubiquitinated proteins. The *rpn11-1* (*mpr1-1*) mutant contains a frameshift near the carboxyl terminus (40), which results in the replacement of the terminal 31 amino acids with nine nonnative residues. This well characterized temperature-sensitive mutant (20, 40) displays growth and proteolytic deficiencies (21, 40), as well as a mitochondrial defect (20). The *rpn11*^{AXA} mutant contains changes in the MPR1-PAD1-N terminus (MPN) domain and does not support viability, although its biochemical properties can be examined in an *rpn11-1* mutant (21).

The significant proteolytic and growth defects of *rpn11-1* led us to examine proteasome interaction with ubiquitinated proteins and shuttle factors. Proteasomes are structurally defective in *rpn11-1* and show a specific loss of 19 S subunits. Consequently, the low peptidase activity of proteasomes in *rpn11-1* may be due to the diminished stimulatory effect that the 19 S regulatory particle is known to exert. These proteasomes also showed significantly reduced interaction with multiubiquitinated proteins. In contrast, proteasomes containing the catalytically inactive rpn11^{AXA} protein are structurally sound and bind very high levels of multiubiquitinated proteins due to defective deubiquitination (21). These results show that the interaction between ubiquitinated proteins and the proteasome can be uncoupled from the subsequent steps involving deubiquitination and degradation.

The carboxyl-terminal 39 residues of Rpn11 can function in *trans* to partially restore proteasome assembly. GST-C^{Rpn11} improved growth of *rpn11-1* at the non-permissive temperature and increased survival in the presence of translational inhibitors. Additionally, normal resistance to UV light was restored, and the degradation of a proteolytic substrate was improved. Direct binding studies failed to reveal any interaction between FLAG-rpn11-1 and GST-C^{Rpn11}, indicating that suppression is not achieved by dimerization of these protein sequences (data not shown and Ref. 22). Because rpn11-1 protein is catalytically active but destabilizes proteasomes, we propose that the carboxyl terminus promotes proteasome stability, consistent with previous reports showing its requirement for Rpn11 function (21–23).

Multiubiquitinated proteins accumulated in *rpn11-1* but were not detected at correspondingly high levels in the proteasome. However, high levels of ubiquitinated proteins were co-purified with shuttle factors. Proteasomes purified from *rpn11-1* contained reduced levels of the 19 S subunit Rpn1, which forms the primary interaction with shuttle factors (38). This provides an explanation for the reduced interaction between shuttle factors and proteasomes in *rpn11-1*. In contrast, the high levels of multiubiquitinated proteins in proteasomes in *rpn11*^{AXA} indicate that shuttle factors can bind intact proteasomes, even if they are catalytically inactive for deubiquitination.

Our results suggest that the primary defect of *rpn11-1* is the instability of the lid complex rather than a failure to properly assemble proteasomes. Although we cannot disregard an assembly defect, our model is supported by the detection of intact proteasomes in *rpn11-1* following *in vivo* cross-linking (Fig. 3). Rad23 and Rpn10, as well as multiubiquitinated proteins, were readily co-purified with proteasomes from *rpn11-1* following cross-linking.

Lower amounts of Rad23 and Dsk2 were detected in proteasomes isolated from *rpn11-1*, suggesting inefficient delivery of shuttle factors. However, high amounts of multiubiquitinated proteins were bound to these shuttle factors. Presumably, multiubiquitinated proteins that are not delivered to the proteasome can remain bound to shuttle factors. The increased amount of fully assembled proteasomes in *rpn11*^{AXA} might underlie their favorable interaction with multiubiquitinated proteins. Taken together, these findings suggest that shuttle factors and ubiquitinated proteins may bind proteasomes only after the lid subcomplex has assembled with the base-20 S complex. The release of shuttle factors from proteasomes could be linked to the disassembly of multiubiquitin chains, which was shown to be coupled to substrate degradation (21).

The overall abundance of proteasome subunits is not markedly affected in *rpn11*^{AXA}, as judged by immunoblotting (Fig. 1). However, both in-gel assays and immunoprecipitated proteasomes showed higher chymotryptic activity in *rpn11*^{AXA}. Because high levels of multiubiquitinated proteins are bound to proteasome in *rpn11*^{AXA}, we speculate that peptidase activity might be positively affected by interaction with proteolytic substrates, but their degradation requires deubiquitination (21).

The addition of SDS did not stimulate the peptidase activity of proteasomes purified with either FLAG-Rad23 or FLAG-Dsk2 from *rpn11-1* (Fig. 7*C*). Because shuttle factors interact with the 19 S complex, these results support the model that lower amounts of the 20 S particle were co-purified with shuttle factors from *rpn11-1*. Based on these findings, it will be of interest to determine how the level of proteasome assembly affects substrate turnover and whether deubiquitination regulates the release of shuttle factors from the proteasome.

Acknowledgments—Members of the laboratory are thanked for critical review of the manuscript. We thank Drs. Dohmen (University of Cologne), Verma (California Institute of Technology), Deshaies (California Institute of Technology), Enenkel (Humboldt University), Skowyra (St. Louis University), and Peltz (UMDNJ), for plasmids, strains, and antibodies.

REFERENCES

1. Glickman, M. H., and Ciechanover, A. (2002) *Physiol. Rev.* **82,** 373–428
2. Rosenzweig, R., and Glickman, M. H. (2008) *Biochem. Soc. Trans.* **36,**

807–812
3. Ramos, P. C., and Dohmen, R. J. (2008) *Structure* **16,** 1296–1304
4. Le Tallec, B., Barrault, M. B., Courbeyrette, R., Guérois, R., Marsolier-Kergoat, M. C., and Peyroche, A. (2007) *Mol. Cell* **27,** 660–674
5. Kusmierczyk, A. R., Kunjappu, M. J., Funakoshi, M., and Hochstrasser, M. (2008) *Nat. Struct. Mol. Biol.* **15,** 237–244
6. Saeki, Y., Toh-E., A., Kudo, T., Kawamura, H., and Tanaka, K. (2009) *Cell* **137,** 900–913
7. Roelofs, J., Park, S., Haas, W., Tian, G., McAllister, F. E., Huo, Y., Lee, B. H., Zhang, F., Shi, Y., Gygi, S. P., and Finley, D. (2009) *Nature* **459,** 861–865
8. Park, S., Roelofs, J., Kim, W., Robert, J., Schmidt, M., Gygi, S. P., and Finley, D. (2009) *Nature* **459,** 866–870
9. Murata, S., Yashiroda, H., and Tanaka, K. (2009) *Nat. Rev. Mol. Cell Biol.* **10,** 104–115
10. Le Tallec, B., Barrault, M. B., Guérois, R., Carré, T., and Peyroche, A. (2009) *Mol. Cell* **33,** 389–399
11. Kaneko, T., Hamazaki, J., Iemura, S., Sasaki, K., Furuyama, K., Natsume, T., Tanaka, K., and Murata, S. (2009) *Cell* **137,** 914–925
12. Funakoshi, M., Tomko, R. J., Jr., Kobayashi, H., and Hochstrasser, M. (2009) *Cell* **137,** 887–899
13. Glickman, M. H., Rubin, D. M., Fu, H., Larsen, C. N., Coux, O., Wefes, I., Pfeifer, G., Cjeka, Z., Vierstra, R., Baumeister, W., Fried, V., and Finley, D. (1999) *Mol. Biol. Rep.* **26,** 21–28
14. van Nocker, S., Sadis, S., Rubin, D. M., Glickman, M., Fu, H., Coux, O., Wefes, I., Finley, D., and Vierstra, R. D. (1996) *Mol. Cell Biol.* **16,** 6020–6028
15. Díaz-Martínez, L. A., Kang, Y., Walters, K. J., and Clarke, D. J. (2006) *Cell Div.* **1,** 28
16. Funakoshi, M., Sasaki, T., Nishimoto, T., and Kobayashi, H. (2002) *Proc. Natl. Acad. Sci. U.S.A.* **99,** 745–750
17. Lambertson, D., Chen, L., and Madura, K. (1999) *Genetics* **153,** 69–79
18. Elsasser, S., Chandler-Militello, D., Müller, B., Hanna, J., and Finley, D. (2004) *J. Biol. Chem.* **279,** 26817–26822
19. Verma, R., Oania, R., Graumann, J., and Deshaies, R. J. (2004) *Cell* **118,** 99–110
20. Rinaldi, T., Ricordy, R., Bolotin-Fukuhara, M., and Frontali, L. (2002) *Gene* **286,** 43–51
21. Verma, R., Aravind, L., Oania, R., McDonald, W. H., Yates, J. R., 3rd, Koonin, E. V., and Deshaies, R. J. (2002) *Science* **298,** 611–615
22. Rinaldi, T., Hofmann, L., Gambadoro, A., Cossard, R., Livnat-Levanon, N., Glickman, M. H., Frontali, L., and Delahodde, A. (2008) *Mol. Biol. Cell* **19,** 1022–1031
23. Rinaldi, T., Pick, E., Gambadoro, A., Zilli, S., Maytal-Kivity, V., Frontali, L., and Glickman, M. H. (2004) *Biochem. J.* **381,** 275–285
24. Gietz, R. D., and Sugino, A. (1988) *Gene* **74,** 527–534
25. Chuang, S. M., and Madura, K. (2005) *Genetics* **171,** 1477–1484
26. Bachmair, A., Finley, D., and Varshavsky, A. (1986) *Science* **234,** 179–186
27. Ortolan, T. G., Tongaonkar, P., Lambertson, D., Chen, L., Schauber, C., and Madura, K. (2000) *Nat. Cell Biol.* **2,** 601–608
28. Glickman, M. H., Rubin, D. M., Fried, V. A., and Finley, D. (1998) *Mol. Cell Biol.* **18,** 3149–3162
29. Groll, M., Bajorek, M., Köhler, A., Moroder, L., Rubin, D. M., Huber, R., Glickman, M. H., and Finley, D. (2000) *Nat. Struct. Biol.* **7,** 1062–1067
30. Braun, B. C., Glickman, M., Kraft, R., Dahlmann, B., Kloetzel, P. M., Finley, D., and Schmidt, M. (1999) *Nat. Cell Biol.* **1,** 221–226
31. Smith, D. M., Chang, S. C., Park, S., Finley, D., Cheng, Y., and Goldberg, A. L. (2007) *Mol. Cell* **27,** 731–744
32. Köhler, A., Cascio, P., Leggett, D. S., Woo, K. M., Goldberg, A. L., and Finley, D. (2001) *Mol. Cell* **7,** 1143–1152
33. Chen, L., and Madura, K. (2002) *Mol. Cell Biol.* **22,** 4902–4913
34. Schauber, C., Chen, L., Tongaonkar, P., Vega, I., Lambertson, D., Potts, W., and Madura, K. (1998) *Nature* **391,** 715–718
35. Bertolaet, B. L., Clarke, D. J., Wolff, M., Watson, M. H., Henze, M., Divita, G., and Reed, S. I. (2001) *Nat. Struct. Biol.* **8,** 417–422
36. Chen, L., Shinde, U., Ortolan, T. G., and Madura, K. (2001) *EMBO Rep.* **2,** 933–938
37. Biggins, S., Ivanovska, I., and Rose, M. D. (1996) *J. Cell Biol.* **133,** 1331–1346
38. Elsasser, S., Gali, R. R., Schwickart, M., Larsen, C. N., Leggett, D. S., Müller, B., Feng, M. T., Tübing, F., Dittmar, G. A., and Finley, D. (2002) *Nat. Cell Biol.* **4,** 725–730
39. Raasi, S., and Pickart, C. M. (2003) *J. Biol. Chem.* **278,** 8951–8959
40. Rinaldi, T., Ricci, C., Porro, D., Bolotin-Fukuhara, M., and Frontali, L. (1998) *Mol. Biol. Cell* **9,** 2917–2931